High Energy Density Physics 7 (2011) 84–90

Contents lists available at ScienceDirect

High Energy Density Physics

journal homepage: www.elsevier.com/locate/hedp

Influence of ordered structures on electrical conductivity and XANES from warm to hot dense matter

Jiayu Dai, Yong Hou, Jianmin Yuan*

Department of Physics, College of Science, National University of Defense Technology, Changsha 410073, People's Republic of China

ARTICLE INFO

Article history:
Received 12 February 2011
Accepted 12 February 2011
Available online 22 February 2011

Keywords:
Warm dense matter
QLMD
Ionic structures
XANES
Electrical conductivity

ABSTRACT

The detailed ionic structure of matter from the warm to the hot dense matter regime and its influence on the electrical conductivity and X-ray absorption near-edge spectroscopy (XANES) is studied using the method of quantum Langevin molecular dynamics (QLMD). It is found that the local ordered structures play a pivotal role in the conductivity and XANES when the ionic structure of the matter is transformed from long-range to medium-short-range order and finally to disorder as the temperature increases. Local short-range ordered structures such as chains and circles appear at high temperatures. For a given macroscopic density-temperature point, the dynamical changes of the atomic configurations in the QLMD simulation give rise to variations in the calculated physical properties, indicating that some dynamical features might be lost in usual static models such as average atom and hypernetted-chain (HNC) models.

1. Introduction

Warm dense matter (WDM), a state with densities near or above solid and having temperatures up to 100 eV, has been attracting much interest because of its specific properties and the importance in the inertial confinement fusion (ICF) [1,2], pulsed radiation heating of solid targets [3–6], and astrophysics [7], etc. The characteristics of partial dissociation, ionization, degeneracy and strong coupling [8] in WDM are difficulties that must be considered when attempting to provide accurate simulations. Models have developed to resolve the complexity in this regime, and many semi-classical methods such as Thomas–Fermi molecular dynamics (TFMD) [9], orbital-free molecular dynamics (OFMD) [10], and average atom molecular dynamics (AAMD) [11] have been constructed. However, the most reliable and widely used model is the quantum molecular dynamics (QMD) method, because of its use of ionic potentials generated *ab initio* and its accurate treatment of electrons [7,12–16]. In addition, many physical properties such as equation of state (EOS), optical absorption [17,18], electrical conductivity [13] and thermal conductivity [19] can be obtained through the use of QMD simulations. In particular, a model of quantum Langevin molecular dynamics (QLMD) was developed very recently [20,21], in which the electron-ion collisions induced friction (EI-CIF) was introduced. This model solves the numerical problems in QMD at high temperature, and extends these first principles calculations into the regime of high energy density physics (HEDP). Finally, QLMD has been successfully applied to determine the EOS of solar-interior [22].

The expensive computational cost is the biggest obstacle to applying QMD and QLMD in warm and hot dense matter regime. Thus, static models such as average atoms (AA) [23,24] and hypernetted-chain (HNC) [25,26] were usually employed. However, QMD or QLMD should be used as a benchmark because the static models do not provide reliability in warm and hot dense regime. Furthermore, in the static models, an ionic structure is statistically averaged, and then the physical quantities are calculated. This leads to the comment that the fluctuations of ionic structures in molecular dynamics will lead to fluctuations of physical quantities, which and even the average physical quantities may be not equal to those from static models.

The coupling parameter Γ and degenerate parameter θ defines the state of the matter [8], where $\Gamma = Z^{*2}/(k_B T a)$, and $\theta = T/T_F$. Here, T represents the system temperature, k_B the Boltzmann constant, a the mean ionic sphere radius defined as $a = (3/4\pi n_i)^{1/3}$, Z^* the average ionization degree, n_i the ionic number density, and $T_F = (3\pi^2 n_e)^{2/3}/2$ is the Fermi temperature (n_e is the electron number density). It is believed that the static model can work well when Γ is not large compared to unity [22,26]. However, there is no direct physical evidence that can prove it. For the strongly coupled matter molecular dynamics simulations are often employed because of complex ionic configurations and the strong interaction between ions. Since the electronic distribution is

* Corresponding author.
E-mail address: jmyuan@nudt.edu.cn (J. Yuan).

1574-1818/$ – see front matter © 2011 Elsevier B.V. All rights reserved.
doi:10.1016/j.hedp.2011.02.002

dependent on the ionic structure, the understanding of the influence of the ionic distributions on the physical quantities is necessary.

Generally, two techniques, X-ray absorption near-edge spectroscopy (XANES) [5,27–30] and electrical dc conductivity [13,31,32], can be adopted to diagnose the density-temperature state of dense matter. Thus, the calculation of accurate results becomes important. It has been proved that QMD is reliable for the calculation of these properties, and can describe the ionic structures. It could be easily imagined that the whole ionic structures would transform from long-range order to disorder with the increase of temperature. Using QLMD, it is possible to understand the ionic structures from warm to hot dense matter, and answer the question how the transition from an ordered state affects the XANES and the electrical conductivity. In this way, the applicability of the static models at different conditions could become better understood.

2. Theory

The description of QLMD can be found in Ref. [20–22]. From the density functional theory (DFT), one can calculate the electronic structure as well as the electrical dc conductivity and XANES. The electrical conductivity can be obtained from the Kubo-Greenwood formula [33,34], where the electron-atom, electron-ion, and electron–electron interactions are included. The Kubo-Greenwood formula for the electrical conductivity as a function of the frequency ω can be written as

$$\sigma(\omega) = \frac{2\pi e^2\hbar^2}{3m^2\omega\Omega}\sum_k W(k)\sum_{i,j}\left(f_i^k - f_j^k\right)\Big| \left\langle\psi_i^k\middle|\hat{v}\middle|\psi_j^k\right\rangle\Big|^2\delta\left(E_j^k - E_i^k - \hbar\omega\right) \quad (1)$$

where Ω is the volume of the supercell, e and m are the electron charge and mass, ψ_i^k and E_i^k are the wave function and energy for the i_{th} band at a particular k point in the Brillouin zone, $f_{i\widehat{\ }}^k$ is the corresponding Fermi weight and $W(k)$ is the weight factor, v is the velocity operator. The δ function is broadened by using Gaussian function, and the broadening parameter can be chosen according to the rule in Ref. [13]. $\sigma(\omega)$ are the optical absorption spectra at low frequency, and in particular, the value of $\sigma(0)$ is the electrical dc conductivity at $\omega = 0$.

For the calculation of XANES, one first needs to obtain the cross sections. In the framework of the single electron approximation, the cross section is defined as

$$\eta(\omega) = 4\pi^2\alpha_0\hbar\omega\sum_f |M_{i\to f}|^2\delta\left(E_f - E_i - \hbar\omega\right) \quad (2)$$

where $\hbar\omega$ is the photon energy, α_0 is the fine-structure constant, and $|M_{i\to f}|$ are the transition amplitudes between an initial core state $|\psi_i\rangle$ with energy E_i, localized on the absorbing atom site, and an all electron final state $|\psi_f\rangle$ with energy E_f:

$$|M_{i\to f}| = \left\langle\psi_f\middle|\widehat{\zeta}\middle|\psi_i\right\rangle \quad (3)$$

where $\widehat{\zeta}$ is a transition operator coupling initial and final states. Up to the electric quadrupole approximation, $\widehat{\zeta}$ can be described by the formula of $\widehat{\varepsilon}\cdot r(1 + (i/2)k\cdot r)$, where $\widehat{\varepsilon}$ and k are the polarization vector and the wave vector of the photon beam, respectively. Taillefumier et al. developed a reciprocal-space pseudopotential scheme for calculating XANES based on DFT [35,36]. In their approach, once the charge density is known, it is not necessary to calculate empty bands to describe very high energy features of the spectrum. In this work, we also use this method to calculate the XANES of carbon embedded in dense hydrogen.

3. Computational details

The properties of the dense hydrogen have always attracted much attention due to its importance in many fields such as superconductor [37,38]. In this work, we firstly study the transition of ionic structure and the electrical conductivity with the increase of temperature for dense hydrogen at a density of 10 g/cm^3. Five temperature points are adopted, which are 1000 K, 1 eV, 10 eV, 100 eV and 550 eV. The atomic radius is about 0.34 Å for hydrogen at 10 g/cm^3, and thus a norm-conserving Coulombic pseudopotential with radius cutoff of 0.01 Å is constructed. Using this pseudopotential, the cutoff for the kinetic energy is 200 Ry to 400 Ry depending on the different temperatures. All calculations are carried out within the framework of finite temperature DFT [39] using the generalized-gradient approximation (GGA) [40]. The temperature dependency of the exchange-correlation functional is not considered here. By using the Γ point only for the representation of the Brillouin zone and 256 particles in a cubic supercell with periodic boundary conditions, ionic structures are investigated by QLMD, which has been incorporated into the Quantum-Espresso package [21,41]. Enough empty bands are used in order to ensure the corresponding band energies higher than 10 k_B T at every temperature point. All these parameters have been examined carefully, and it is found that more k points, more bands, larger energy cutoff, and more particles do not make a significant difference in the results. The time step used for the QLMD is $a_I/(20\sqrt{k_BTM_I})$ [19], where a_I and M_I are the average ionic radius and the ionic mass of the I_{th} ion, respectively. Each temperature point was simulated for at least 1 ps temporal duration to reach thermal equilibrium, with 5000–10000 time steps to form the ensemble information after thermalization.

To calculate the XANES of carbon in dense hydrogen, one hydrogen atom was substituted with a carbon atom in the supercell, and the corresponding lattice constant was enlarged using different densities. All other parameters were similar to dense hydrogen. The XSPECTRA code is used here [42].

4. Results and discussion

4.1. Transition of ordered structures

First, the temperature-dependent ionic structures of the dense hydrogen were investigated. It is well-known that the ions should transform from long-range order at the low temperature to disorder at the high temperature [43]. In order to understand this process, the radial distribution functions (RDF) $g(r)$ at different temperatures are shown in Fig. 1. It is clear that dense hydrogen is an ideal crystal at low temperature of 1000 K, the lowest temperature calculated, when the ions only fluctuate around their equilibrium positions. Statistically this is a long-range ordered structure. With increasing temperature, the long-range order is lost, and the ions exhibit the characteristics of the medium- or short-range order at the temperature of 1 eV. By 10 eV, the ordered structure tends to disappear. Furthermore, when the temperature reaches 100 eV, the dense hydrogen starts to behave like an ideal gases, where the ions are almost moving freely. At the temperature of 550 eV, the RDF is similar to that at 100 eV; however, here the ions act essentially ideal gas-like.

The above characteristics correspond to the ionic coupling parameter Γ with values 488, 44, 4, 0.4 and 0.0077 at the temperatures of 1000 K, 1 eV, 10 eV, 100 eV and 550 eV, respectively, which means the coupling of ions at 100 eV and 550 eV is

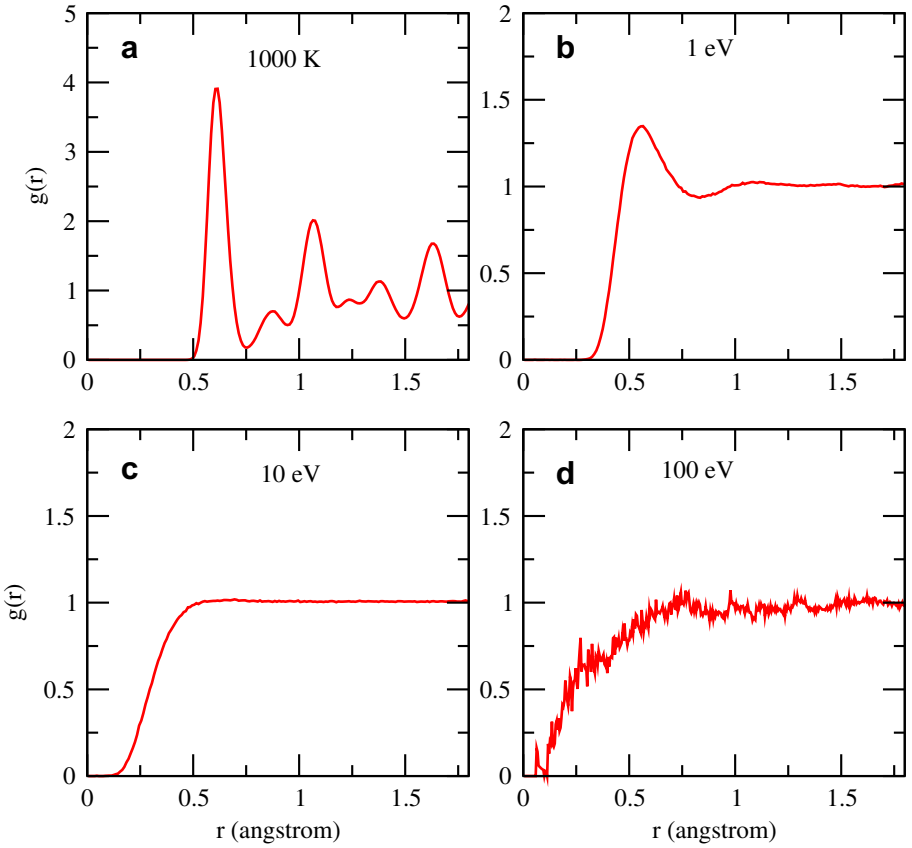

Fig. 1. The RDF of dense hydrogen at a density of 10 g/cm^3 and different temperatures.

weak, resulting in the ideal gas features. However, the RDF just shows us the ionic structures statistically, and the specific details of the local structure and its change around an ion are unknown. In fact, the particular local structure is responsible for the physical models we are using. In order to further explain the detailed short-ordered structures, further analysis has been done to try to reveal the existing short-range ionic structures in warm dense matter. A global-search method is used to explore the detailed structures at different temperatures, and find the number of nearest atoms within a specific distance for every atom. Similar methods are used in the study of metallic glasses [44], where methods such as Voronoi tessellation [45] are adopted. To elaborate we first define the short-range ordered ionic structures as follows:

Single-atom: an atom where there is no nearest atom within the specific distance.

Chain: A chain structure constructed by multiple atoms, whose length is defined by the number of atoms in the chain. In a chain, every atom except the first and last atom of the chain has only two nearest atoms within the specific distance.

Circle: A circle structure constructed by multiple atoms, whose length is represented by the number of atoms in a closed chain. In the chain, every atom has only two nearest atoms within the specific distance.

Cluster: A complex structure constructed by multiple atoms, whose central atom has more than three nearest atoms within the specific distance.

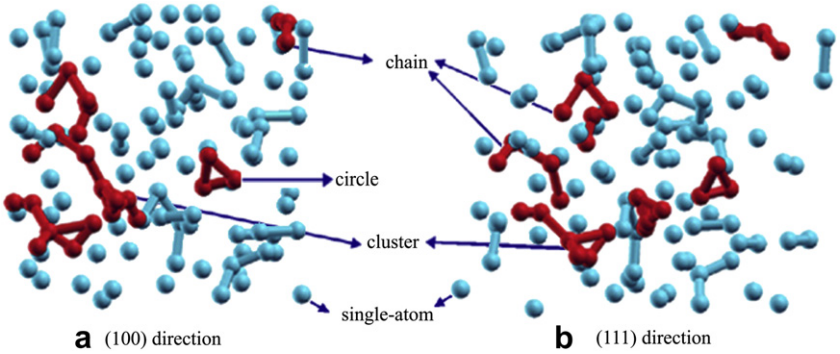

Fig. 2. The detailed ionic structures of one typical configuration at the temperature of 10 eV. (a) and (b) are figures from the view of (100) direction and (111) direction. Some short-ordered structures such as chains, circles and clusters defined in the article are shown in red color. (For interpretation of the references to colour in this figure legend, the reader is referred to the web version of this article.)

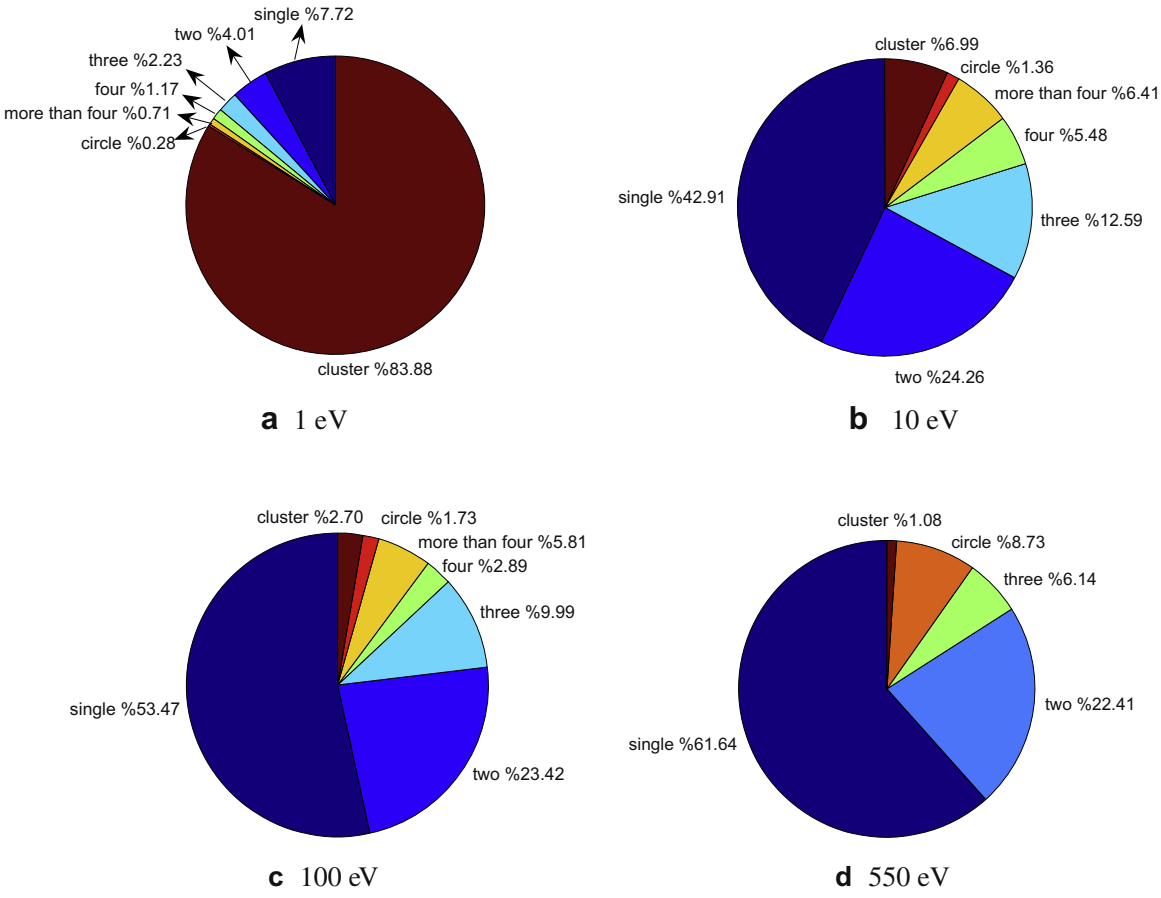

Fig. 3. The percentages of different ordered structures at different temperatures. "single" represents the percentage of the single-atom structure; "two", "three", "four" represent the chain structure with two, three and four atoms, respectively; "more than four" represents the chain structures with more than four atoms; "circle" represents the percentage of all circle structures; and "cluster" represents the percentage of all cluster structures. (a)-(d) are the percentages at the temperatures of 1 eV, 10 eV, 100 eV and 550 eV, respectively.

By these definitions, the details of the ionic structures during the molecular dynamics simulations can be quantified, and thus can supply direct evidence for the static models. The existence of cluster structure indicates that the interactions between multiple ions are important, where the semiclassical models including single-body, two-body and three-body interactions are not valid. The percentages of different structures for all atoms are used to show this information, and more than 5000 time steps are averaged. We define the specific distance, i.e., the cutoff, as the position of the first peak of the RDF at low temperatures or the position of the largest value of the RDF at high temperatures. In order to understand the short-range ordered structures defined here, some typical ordered structures of one typical configuration at the temperature of 10 eV are shown in Fig. 2, where two complex clusters, one circle with three atoms, and three chains with the lengths of 3, 4 and 5 atoms are visualized by red color. Additionally, there are many "single-atom" structures, and there are some chains constructed of only two or three atoms. Similar ordered structures are shown for different times and different temperatures, which will be statistically averaged.

At the temperature of 1000 K, the ions statistically exhibit long-range order, and thus the complex local cluster structures take up 100%. At 1 eV, the ions show medium- or short-range order, and thus the cluster structures are dominant, taking up about 84%, as shown in Fig. 3(a). In this case, other structures such as chains are not important, so that semiclassical models based on two-body or three-body interactions are not appropriate. With increasing temperature, the ordered structures disappear gradually, and the occurrence of complex cluster structures diminish. At the temperature of 10 eV, the cluster structures only take up about 7%, as shown in Fig. 3(b). At 10 eV other chain-like structures are dominant, and thus the semiclassical models such has HNC can provide reasonable results. However, it should be noticed that the chains are the most important ingredient in the system, and thus the single atomic models will not be valid. When the temperature reaches 100 eV, the ionic parameter is 0.4, indicating the interactions between ions are not strong. This corresponds to the structures shown in Fig. 3(c), where the single-atom and two or three-body structures are dominant, and the cluster structures decrease further. Finally, when the temperature is 550 eV, the ions behave much like an ideal gas, whose ionic parameter is about 0.077. The details of the structures are shown in Fig. 3(d), where there is no chain with length of more than four. Furthermore, the analysis show that the length of all circles is only three, indicating that the single, two- and three-body structures comprise 99% of the atoms. Most one and bi-atomic models [46] can be applied validly and will yield the correct physical quantities in these conditions.

4.2. Electrical conductivity

Different ionic ordered structures would lead to different electronic physical quantities. Here, we study the change of the electrical dc conductivity and XANES. For the calculation of the electrical conductivity, $4\times4\times4$ k points and 0.2 eV Gaussian broadening parameter are adopted in all cases, which have been tested to ensure convergence. First, our model was compared with

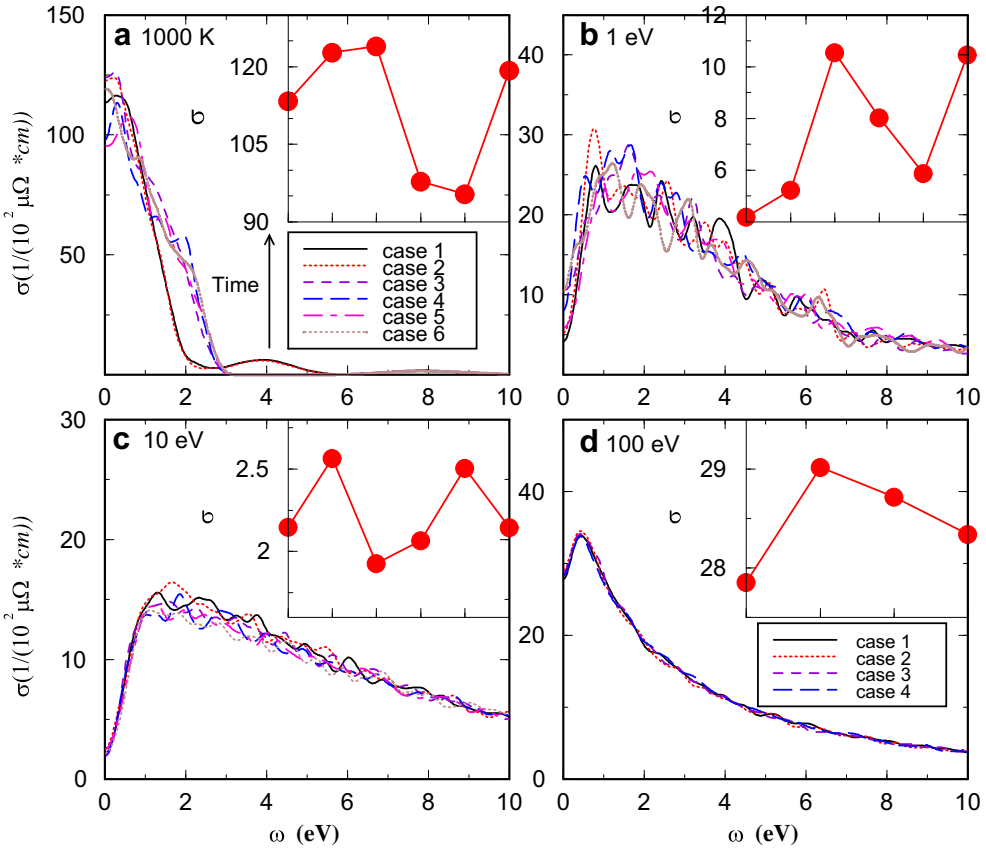

Fig. 4. The optical absorption at low frequency and electrical dc conductivity (inset figure) at different temperatures. (a)-(d) are the representation of the temperatures of 1000 K, 1 eV, 10 eV and 100 eV, respectively.

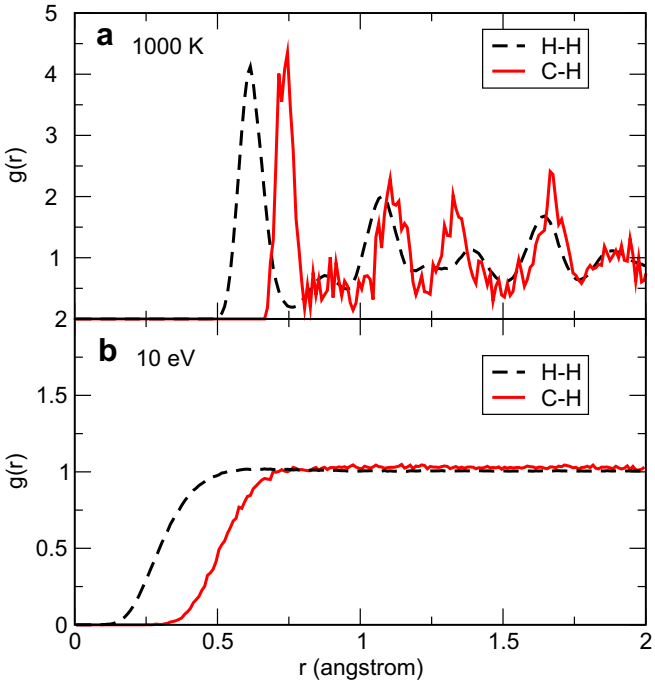

Fig. 5. The RDF of one carbon atom embedded in dense hydrogen at a density of 10 g/cm^3 and temperatures of 1000 K (a) and 10 eV (b).

previous results for hydrogen presented in Ref. [13,16,17] and all the comparisons show agreement.

For long-range order at 1000 K, the conductivity is shown in Fig. 4(a). Six different configurations (6 cases) during the molecular dynamics simulation after thermalization were used to compare the conductivity, and the time step between cases is 0.1 ps. It is clear that the optical absorption spectra at low frequency differ. Especially at frequency zero, i.e., the dc conductivities of different cases are much different. From the inset plot in Fig. 4(a), we can find that the fluctuation of the electrical dc conductivity is within 20%. In fact, although the system is statistically long-range ordered, the ions fluctuate at each time step of the molecular dynamics simulation, which is consistent with the physical behavior of the system. From the viewpoint of instantaneousness, the ionic structure is not exactly long-range ordered, as it is a little disordered. The fluctuation of ionic positions leads to the fluctuation of the electrical conductivity, and therefore, the statistical models may give results with large uncertainties.

At the temperature of 1 eV, the system becomes medium- or short-range ordered, and the optical properties and the conductivities for 6 configurations are shown in Fig. 4(b). The largest fluctuation between different cases is now more than 50%, indicating much violent fluctuation of the ionic structures. It is very interesting that the dc conductivity is much smaller than that at 1000 K. This can be explained by the breakdown of the long-range order at 1 eV, as shown in Fig. 1(b) and Fig. 3(a), giving an indication that more ordered structures result in a larger conductivity. This is further verified when we analyze the properties at 10 eV, where the electrical conductivities for 6 different cases are shown in Fig. 4(c). At 10 eV, the medium range ordered structures seem to disappear,

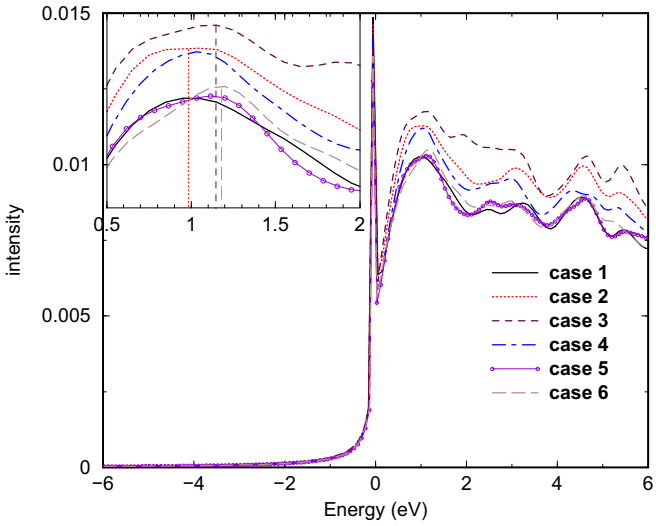

Fig. 6. XANES of C in dense hydrogen at the temperature of 1000 K. In the inset plot, the second peak of different cases are shown.

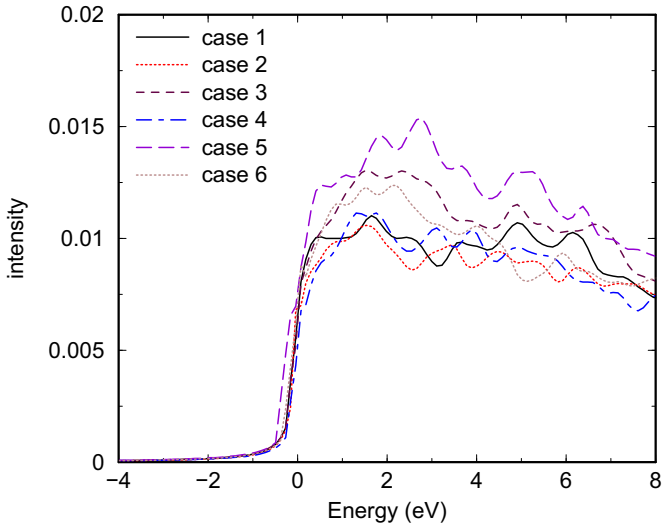

Fig. 8. XANES of C in dense hydrogen at the temperature of 10 eV.

as shown in Fig. 1(c) and Fig. 3(b), and thus the electrical dc conductivity is smaller than that at 1 eV. It is noted that the fluctuation of conductivity at 10 eV is no more than 25%, which is also smaller than that at 1 eV; however, this is still a significant fluctuation. This tells us there should be some short-range ordered structures at the temperature of 10 eV, which is in agreement with the detailed structures in Fig. 3(b). When the temperature is increased to 100 eV the trend is altered, as the conductivity is now larger than those at 1 eV and 10 eV, which is due to the high temperature. Nevertheless, the electrical conductivities of 4 different cases at 100 eV are shown in Fig. 4(d), whose optical properties at low frequency and electrical dc conductivities at different times are much similar. In fact, the coupling parameter Γ is only about 0.4 for this case and the interactions between multiple ions are not dominant, as shown in Fig. 3(c). Therefore, the fluctuation of ionic structure does not play a significant role in the physical quantities. When the temperature is 550 eV, the fluctuation of electrical dc conductivity is even much smaller than that at 100 eV, which is consistent with the structural analyses in Fig. 3(d).

4.3. XANES

For the XANES analysis, results at two temperatures clearly show the influence of ordered structures on the optical absorption. In order to obtain the complete spectral characteristics, the broadening parameter in XANES calculation is 0.1–0.3 eV. The system should be long-range ordered at the temperature of 1000 K, and disordered at 10 eV, as shown in Fig. 5. It is noticed that for the C–H structures, the order transition is also obvious. At low temperature the carbon atom should bond with the close hydrogen atoms, and the environment around C will be different for different time steps. Thus, the XANES will fluctuate, as shown in Fig. 6, where it is very clear that the positions of the second peak for different cases are shifted. For example, for the case 2, case 3, and case 6, the shifts of the positions (E_k) of the peaks are:

$$\begin{cases} E_k(\text{case3}) - E_k(\text{case2}) = 0.18\text{eV} \\ E_k(\text{case6}) - E_k(\text{case2}) = 0.2\text{eV} \\ E_k(\text{case6}) - E_k(\text{case3}) = 0.02\text{eV} \end{cases} \tag{4}$$

The reason for these shifts are due to the ionic structures of carbon, as shown in Fig. 7,where the number of C–H bonds within a specific radius is distinct. For example, for case 2, there are six C–H bonds, and for case 3 and case 6, there are eight C–H bonds. This means that the electronic environment of C atom is different between case 2 and the other two cases. It is well-known that XANES is sensitive to the local environment of the atom, which induces the shifts of different peaks.

When the temperature increases to 10 eV, the structure of the peak for absorption spectra disappears (shown in Fig. 8), which also

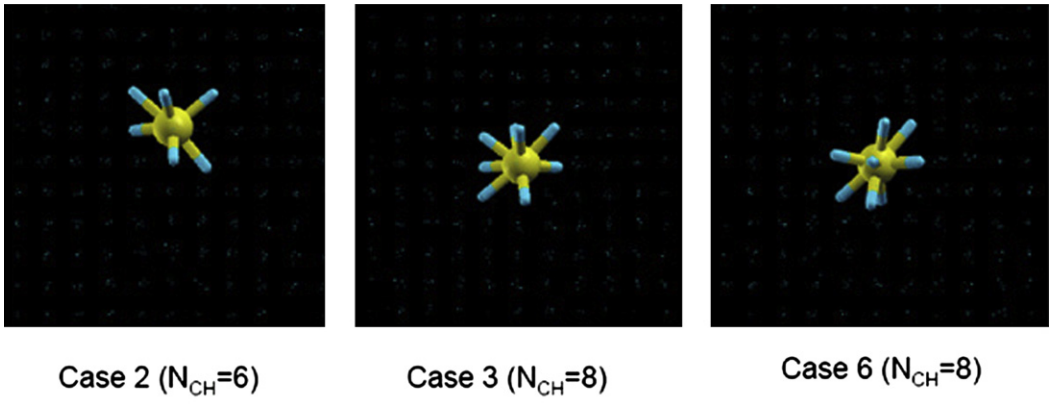

Fig. 7. Three typical ionic structures of case 2, 3,6 used in Fig. 6 at the temperature of 1000 K.

indicates the disordered structure corresponding to the RDF in Fig. 5(b). However, it is noticed that the K-edges of carbon for different cases are found to shift. This shift should result from the short-range ordered structures, as described above. By observing this shift one might be able to develop an alternative diagnostic for the different structures at different times if the experimental techniques can satisfy the requirement of ultra-fast resolvability. From the RDF in Fig. 5, one can find that the average volume occupied by an ion is proportional to its charge value as assumed in the AA model before [47].

5. Conclusion

In conclusion, the detailed ionic structure of dense plasmas transforms from long-range order to medium- or short-range order to disorder as the system makes the transition from cold dense matter through warm dense matter to hot dense matter. These ordered structures have significant influence on the electrical dc conductivity, optical absorption at low frequency and XANES. After analyses, we can draw some conclusions:

First, the ordered structures are broken when temperature is high enough, and the chain-like structures occur increasingly with the increase of temperature.

Second, the ordered structures can enhance the electrical conductivity of dense hydrogen.

Third, the electrical conductivity and XANES fluctuate at relatively low temperature where the coupling of the ions is strong, and this fluctuation disappears when the system acts like ideal gases. Furthermore, these fluctuations present a question for all statistical models: whether the physical quantities derived from statistical models are consistent with the physical behavior determined using the results from molecular dynamics simulations?

Acknowledgments

We thank Professor Zengxiu Zhao and Paolo Giannozzi for helpful discussions. This work is supported by the National Natural Science Foundation of China under Grant Nos. 10734140 and 60921062, the National Basic Research Program of China (973 Program) under Grant No. 2007CB815105. Calculations are carried out at the Research Center of Supercomputing Application, NUDT.

References

[1] J.D. Lindl, Inertial Confinement Fusion. Springer Verlag, New York, 1998.
[2] S. Atzeni, J. Meyer-ter-Vehn, The Physics of Inertial Fusion. Clarendon Press, Oxford, 2004.
[3] U. Zastrau, C. Fortmann, R.R. Fäustlin, et al., Phys. Rev. E 78 (2008) 066406.
[4] P.K. Patel, A.J. Mackinnon, M.H. Key, et al., Phys. Rev. Lett. 91 (2003) 125004.
[5] A. Mančić, A. Lévy, M. Harmand, et al., Phys. Rev. Lett. 104 (2010) 035002.
[6] A. Mančić, J. Robiche, P. Antici, et al., High Energy Den. Phys. 6 (2010) 21.
[7] W. Lorenzen, B. Holst, R. Redmer, et al., Phys. Rev. Lett. 102 (2009) 115701.
[8] S. Ichimaru, Rev. Mod. Phys. 54 (1982) 1017.
[9] F. Lambert, J. Clerouin, G. Zerah, et al., Phys. Rev. E 73 (2006) 016403.
[10] F. Lambert, et al., Europhys. Lett. 75 (2006) 681.
[11] Y. Hou, J. Yuan, Phys. Rev. E 79 (2009) 016402.
[12] L. Collins, I. Kwon, J. Kress, N. Troullier, D. Lynch, Phys. Rev. E 52 (1995) 6202.
[13] M.P. Desjarlais, J.D. Kress, L.A. Collins, Phys. Rev. E 66 (2002) 025401 (R).
[14] S. Mazevet, M.P. Desjarlais, L.A. Collins, J.D. Kress, N.H. Magee, Phys. Rev. E 71 (2005) 016409.
[15] D.A. Horner, J.D. Kress, L.A. Collins, Phys. Rev. B. 77 (2008) 064102.
[16] B. Holst, R. Redmer, M.P.P. Desjarlais, Phys. Rev. B. 77 (2008) 184201.
[17] L. Collins, S.R. Bickham, J.D. Kress, et al., Phys. Rev. B. 63 (2001) 184110.
[18] S. Mazevet, G. Zérah, Phys. Rev. Lett. 101 (2008) 155001.
[19] V. Recoules, F. Lambert, A. Decoster, B. Canaud, J. Clérouin, Phys. Rev. Lett. 102 (2009) 075002.
[20] J.Y. Dai, J.M. Yuan, Europhys. Lett. 88 (2009) 20001.
[21] J.Y. Dai, Y. Hou, J.M. Yuan, Phys. Rev. Lett. 104 (2010) 245001.
[22] J.Y. Dai, Y. Hou, J.M. Yuan, Astrophys. J. 721 (2010) 1158.
[23] Y. Hou, F.T. Jin, J.M. Yuan, Phys. Plasmas 13 (2006) 093301.
[24] G. Faussurier, C. Blancard, P. Cossé, P. Renaudin, Phys. Plasmas 17 (2010) 052707.
[25] D.V. Rose, T.C. Genoni, D.R. Welch, R.E. Clark, R.B. Campbell, T.A. Mehlhorn, D.G. Flicker, Phys. Plasmas 16 (2009) 102105.
[26] K. Wunsch, J. Vorberger, D.O. Gericke, Phys. Rev. E 79 (2009) 010201 (R).
[27] D.K. Bradley, J. Kilkenny, S.J. Rose, J.D. Hares, Phys. Rev. Lett. 59 (1987) 2995.
[28] L. Lecherbourg, P. Renaudin, S. Bastiani-Ceccotti, et al., High Energy Den. Phys. 3 (2007) 175e180.
[29] V. Recoules, S. Mazevet, Phys. Rev. B. 80 (2009) 064110.
[30] A. Lévy, F. Dorchies, M. Harmand, et al., Plasma Phys. Control Fusion 51 (2009) 124021.
[31] P. Renaudin, C. Blancard, G. Faussurier, P. Noiret, Phys. Rev. Lett. 88 (2002) 215001.
[32] K.Y. Kim, B. Yellampalle, J.H. Glownia, A.J. Taylor, G. Rodriguez, Phys. Rev. Lett. 100 (2008) 135002.
[33] R.J. Kubo, Phys. Soc. Jpn. 12 (1957) 570.
[34] D.A. Greenwood, Proc. Phys. Soc. Jpn. 71 (1958) 585.
[35] M. Taillefumier, D. Cabaret, A.M. Flank, F. Mauri, Phys. Rev. B. 66 (2002) 195107.
[36] C. Gougoussis, M. Calandra, A.P. Seitsonen, F. Mauri, Phys. Rev. B. 80 (2009) 075102.
[37] N.W. Ashcroft, Phys. Rev. Lett. 21 (1968) 1748.
[38] P. Cudazzo, G. Profeta, A. Sanna, A. Floris, A. Continenza, S. Massidda, E.K.U. Gross, Phys. Rev. Lett. 100 (2008) 257001.
[39] N.D. Mermin, Phys. Rev. 137 (1965) A1441.
[40] J.P. Perdew, K. Burke, M. Ernzerhof, Phys. Rev. Lett. 77 (1996) 3865.
[41] P. Giannozzi, et al., J. Phys. Condens. Matter 21 (2009) 395502.www.quantum-espresso.org.
[42] The XSPECTRA package by C. Gougoussis, M. Calandra, A. Seitsonen, and F. Mauri is available under the GNU license in the current version of the Quantum ESPRESSO package.
[43] D.O. Gericke, K. Wunsch, A. Grinenko, J. Vorberger, J. Phys. Conf. Ser. 220 (2010) 012001.
[44] H.W. Sheng, W.K. Luo, F.M. Alamgir, J.M. Bai, E. Ma, Nature 439 (2006) 419.
[45] J.L. Finney, Nature 266 (1977) 309.
[46] C.S. Meng, Z.X. Zhao, J.M. Yuan, Chin. Phys. Lett. 25 (2008) 2452.
[47] J.M. Yuan, Phys. Rev. E. 66 (2002) 047401.